

COUPLED RANS-VOF MODELLING OF FLOATING TIDAL STREAM CONCEPTS

E. Ransley¹, S. Brown and D. Greaves

Plymouth University
Plymouth, Devon, UK

S. Hindley

Mojo Maritime Ltd.
Falmouth, Cornwall, UK

P. Weston

A&P Group Ltd.
Falmouth, Cornwall, UK

E. Guerrini

Modular Tide Generators Ltd.
Woking, Surrey, UK

R. Starzmann

Schottel Hydro GmbH
Spay/Rhein, Germany

¹Corresponding author: edward.ransley@plymouth.ac.uk

INTRODUCTION

Numerical models are now capable of providing the quantitative description required for engineering analysis. However, for structures such as floating tidal stream devices, the complex nature of the system can rarely be included using existing functionality. Typically key aspects of the system are considered separately or omitted from the analysis completely. This leads to a number of uncertainties in both the power delivery and the survivability of these devices.

To better understand the behaviour of such systems, a coupled Computational Fluid Dynamics (CFD) model, including a floating barge, hybrid-catenary mooring system and the influence of a submerged turbine has been developed and tested at full-scale in conditions based on those at the Perpetuus Tidal Energy Centre (PTEC) site.

Simulations have been performed for a device with and without a turbine installed; in waves and currents, both separately and simultaneously; in order to ascertain the influence each coupled element has on the motion, mooring loads and power delivery of a floating tidal stream concept.

METHODOLOGY

The CFD method utilises the open-source software OpenFOAM® to solve the fully nonlinear, incompressible, Reynolds-Averaged Navier-Stokes (RANS) equations for air and water using the Finite Volume Method (FVM) and a Volume of Fluid (VOF) treatment for the free-surface [1]. The behaviour of the device has been included using a coupled rigid-body solver in combination with a two-way actuator disk turbine model. Laminar flow conditions have been assumed.

The barge and computation mesh design

The buoyant barge is 18m long, 7m wide and 1.5m deep and is based on existing plans with a 'moon-pool' to accommodate a 4mØ SCHOTTEL Instream Turbine (SIT250). The initial concept barge is steel, weighs 60te and has 22te of ballast to position the barge low enough to avoid the majority of the weather. With the 1.32te turbine unit and 10te support structure installed the moon-pool is covered level with the hull.

The computational domain is 320m long, 60m wide and 90m tall. The side walls and seabed are no-slip boundaries with zero gradient conditions on the pressure and volume fraction, α . The background mesh is made of cubic cells with a 1.67m resolution. The region containing the free surface is refined once using octree refinement and the surface of the barge is refined three times. The barge has fixed- and zero-flux boundary conditions for pressure and velocity respectively and a zero gradient condition for α .

Hybrid-catenary mooring model

The mooring system is made up of four lines each consisting of 85m of synthetic line and 150m of chain. The nonlinear nature of each mooring line is included via a 'look-up table' of the reaction force, derived using an OrcaFlex® model with a single line and a fixed anchor node. In this model, the top node was driven over a Cartesian grid, with 0.5m spacing, and at each position the system statics were calculated. Tri-linear interpolation is then used at each time step to find the precise reaction force for each mooring line and apply it to the barge's motion in the form of a 'restraint'. The dynamics of the mooring lines and their interaction with the fluid has not been included.

Two-way coupled, actuator disk-type turbine model

Including fully blade-resolved turbine models in CFD is extremely compute-intensive prohibiting their use in routine design applications (especially for floating devices). Therefore, further additional functionality has been written for OpenFOAM® to allow the presence of a submerged turbine to be included in the CFD model without the need to fully resolve the turbine's blades in the mesh.

An actuator disk-type method has been used, in which the turbine properties are assumed to be wholly described by the radius of the swept area of the turbine and a constant thrust coefficient,

$$C_t = 4a(1 - a) \quad (1)$$

where a is the axial induction factor linking the free-stream velocity, U_∞ , in the axial direction to the instantaneous local velocity, U_T , by

$$\frac{U_\infty}{U_T} = 1 - a \quad (2)$$

The total thrust force, F_T , on the disk is then

$$F_T = \frac{1}{2}AU_\infty^2 C_t \rho = 2AU_{T^*}^2 ((1/(1 - a)) - 1)\rho, \quad (3)$$

where A is the disk area, ρ is the fluid density and U_{T^*} is the difference between U_T and the turbine velocity due to the motion of the barge.

Here, a 'turbine region' made up of cells within a cylindrical region with the same radius and sharing an axis with the turbine is assumed. The local velocity, U_T , is approximated as the ratio of the vector sum of the Gaussian-weighted velocities of cells within this region to the sum of the weights,

$$G = \frac{1}{\sigma\sqrt{2\pi}} \exp\left(-\frac{dx^2}{2\sigma^2}\right) \quad (4)$$

where dx is the perpendicular distance from the turbine and σ is the Gaussian RMS width. The cylindrical region has a total axial length of 4σ with the turbine positioned centrally. The weights are radially uniform. The total thrust force can then be found, using Equation 3, and added to the barge acceleration calculation, at runtime, without any prior knowledge of the incident flow field.

To couple the thrust on the turbine with the subsequent reduction in fluid momentum, a net equal and opposite body force is applied over the turbine region (Figure 1). The body force in each cell is given as the ratio between the total thrust force, F_T , and the Gaussian weighted volume of the cell (using the same weights as in Equation 4). This body force is then applied as an additional source-term in the momentum equations.

This formulation allows the influence of the a

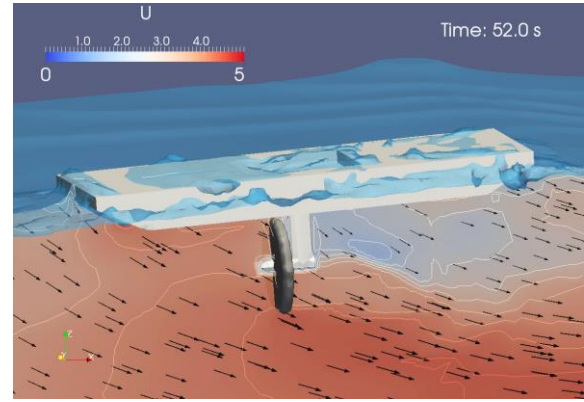


FIGURE 1. SNAPSHOT OF THE LOADED BARGE, IN WAVES AND CURRENTS, SHOWING THE TURBINE REGION, FREE-SURFACE AND FLUID VELOCITIES.

moving turbine to be included at any position and ensures a smooth variation in thrust and applied body force without a complex mesh or re-meshing at runtime. This greatly reduces the CPU effort, compared to blade-resolved models, but, flow structures in close proximity to the turbine blades and any effects due to the blade rotation are not considered. Therefore, although the total thrust on the turbine is theoretically accurate, asymmetric loading or complex wake effects are not captured. Furthermore, any imposed torque, due to power extraction, has not been included in this study.

The model has been validated against the thrust curve of a 4mØ SCHOTTEL turbine (C_t of 0.671) and has been found to predict the total thrust, and the theoretical local velocity, to within 1% (up until the rated flow speed).

Reproducing the environmental conditions at PTEC

The wave and current conditions used in the simulations are based on those at the PTEC site, a proposed demonstration facility to support the development of tidal energy technologies. The site is situated in the English Channel, approximately 2.5 km south of St Catherine's Point on the Isle of Wight. The average depth is ~57m [2].

Observed current data

The Isle of Wight is surrounded by areas of strong tides. From ADCP data, mean spring and neap peak surface flow rates have been estimated at 2.5-2.9ms⁻¹ and 1.3-1.6ms⁻¹ respectively [2]. Current speeds are generally greater immediately below the water's surface than those at depth [2]. However, the measured velocity profiles do not follow either a 7th- or a 10th-power law. Therefore, a fit of the von Karman-Prandtl equation

$$U = \frac{U^*}{k} \ln \frac{Z}{Z_0} \quad (5)$$

has been used to approximate the velocity profile,

where Z is the vertical dimension, U^* is the friction velocity, $k = 0.4$ and Z_0 is the roughness length [3]. For neap tides, $Z_0 = -1.8$, $U^* = 0.09$ matches the data well. For spring tides $Z_0 = -2.24$, $U^* = 0.13$ was an improvement over power law profiles but still has some discrepancies near the seabed.

Wave climate

The English Channel is open to the Atlantic Ocean in the south-west and with dominant south-westerly weather systems the Isle of Wight is open to strong wind-wave and swell conditions. Despite this, the wave climate at the PTEC site is often (22.67% of the time) calm (H_s below 0.5) making the average conditions relatively low [2]. Of more interest are the regular storm events that occur. Under these conditions the device is at its most vulnerable and the impact on the power delivery is likely to be greatest.

The waves in this study are based on a Weibull fit to the wave data from the south-west (the predominant wave direction) with a return period of 1 year. This gave a wave height, H , of 6.1m and a wave period, T , of 9s [2]. The joint probability of spring currents (approximately 1 hour every 14 days) and the 1-in-1 year significant wave height (approximately 3 hours every year),

coinciding for at least one minute, gives this case a return period of around 85 years making it typical of the design limit state of offshore structures.

Numerical wave generation and absorption

The waves and currents are generated using expression-based boundary conditions for the surface elevation and fluid velocity. The 6.1m high, 9s period waves are prescribed using Stokes second-order theory and propagate into initially still water with a half period ramp up of the flow properties. The velocity profile for spring tidal currents is implemented, at time = 0, using Equation 5 ($Z_0 = -2.24$, $U^* = 0.13$) applied to both the wave-maker boundary and the boundary opposite the wave-maker (the outlet).

For the combined wave and current cases, the initial conditions are set using the flow field solution in the current-only cases at $t = 100s$. This allows the barge and flow field to reach a pseudo-steady state before the waves are added using a linear superposition of the two conditions.

Wave (and current) absorption is achieved using the 'relaxation zone' formulation distributed with the additional toolbox 'waves2Foam' [4]. A 30m relaxation zone (RZ) is positioned adjacent to the wave-maker boundary in order to absorb

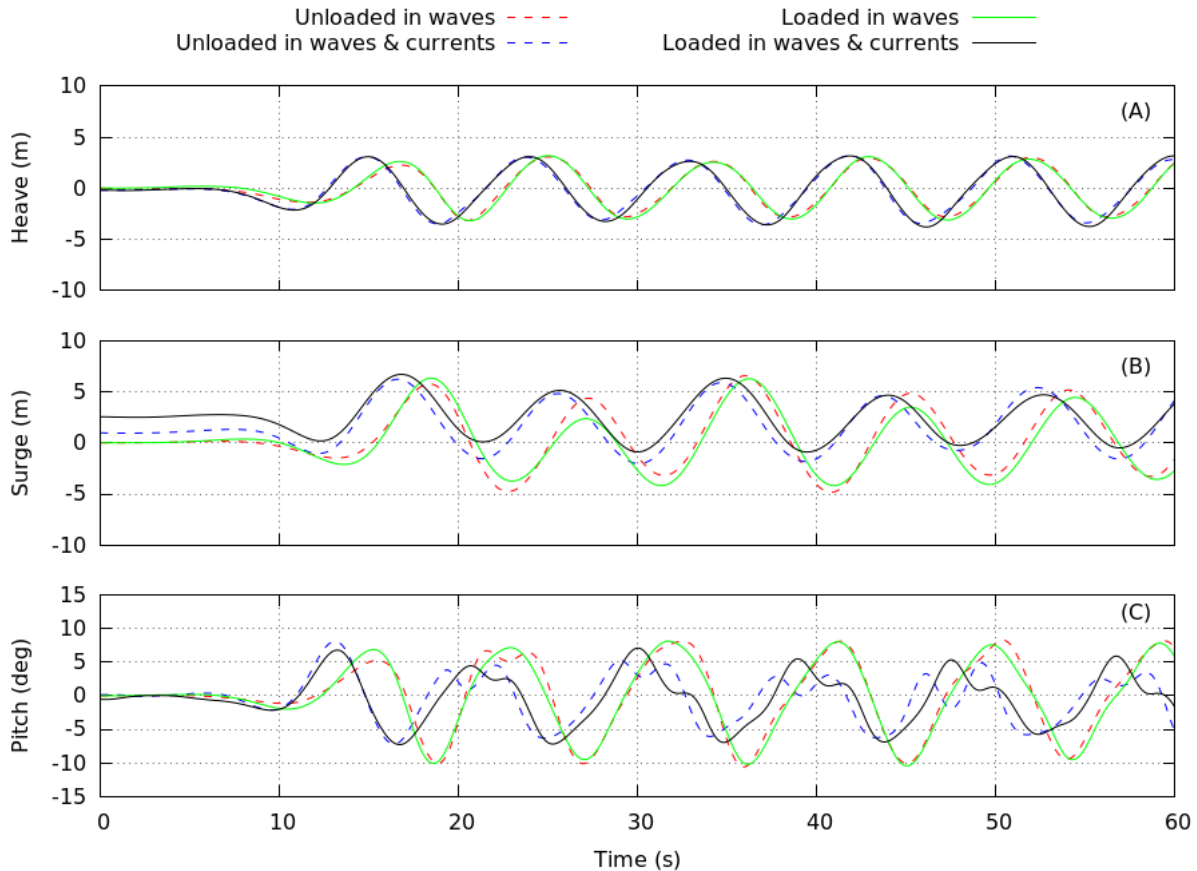


FIGURE 2. TIME SERIES FOR THE HEAVE (A) AND SURGE (B) DISPLACEMENT AND THE PITCH ANGLE (C) OF BOTH THE UNLOADED AND LOADED BARGE IN WAVES AND WAVES AND CURRENTS COMBINED.

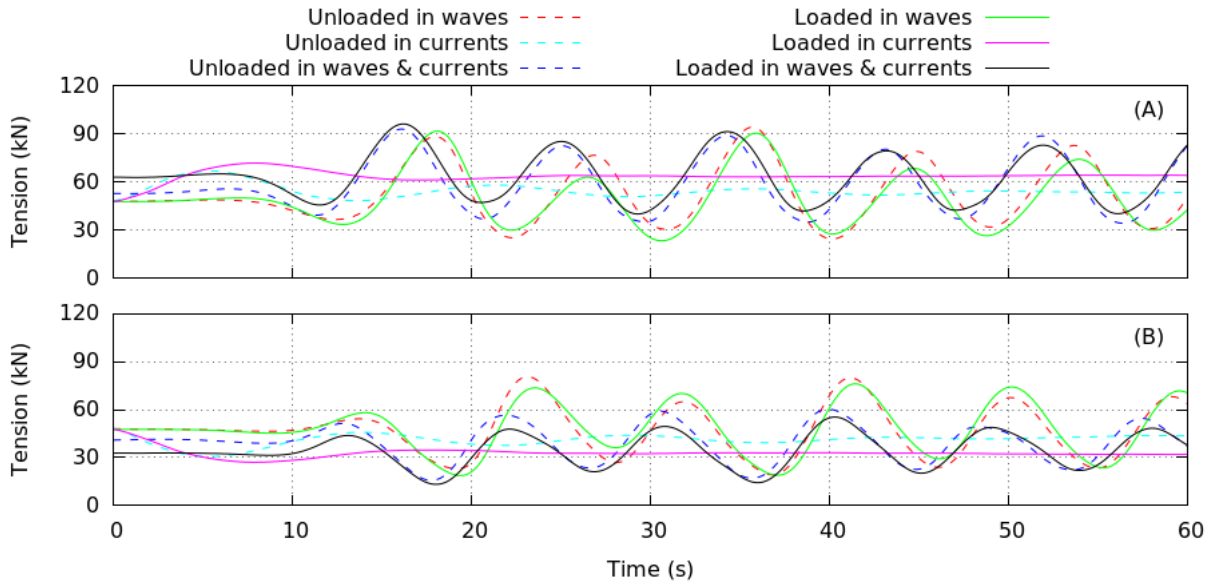


FIGURE 3. TIME SERIES OF THE TOTAL TENSION IN A BOW MOORING LINE (A) AND AN AFT MOORING LINE (B).

waves scattered by the barge. A 240m RZ (~ 2 wavelengths) is positioned adjacent to the outlet boundary. An RZ half this length is sufficient to absorb 99% of the wave [4], however, when including both waves and currents it was found that a far longer RZ was required.

RESULTS AND DISCUSSION

Simulations were run using the barge with (loaded) and without (unloaded) the turbine installed; in waves, currents and waves combined with following currents. 60s of simulation time took ~ 4 hours to run using one node containing two 2.7Ghz, 12-core E5-2697 v2 series processors.

Motion results

Figure 2 shows the position of the centre of mass vertically (A) and in the wave direction (B) as well as the pitch angle (C).

In the combined wave and current cases, the heave displacement displays a $\sim 12\%$ increase in amplitude and a ~ 1.3 s phase shift compared to the wave-only cases. This is believed to be due to an imposed offset in the mooring system, giving a different effective stiffness, and an acceleration of the waves due to the currents (meaning the wave crests arrive earlier despite the barge being further away). The presence of the turbine does not seem to affect the heave displacement.

The surge results (Figure 2B), show the offset due to the currents (most evident at time=0s) with the loaded barge having a greater displacement due to the thrust on the turbine. The surge results show the same phase relationship as the heave, however, in surge, the presence of the turbine acts to reduce the amplitude of oscillation (this was also seen in the current-only cases). Furthermore,

in the combined cases it can be seen that the addition of currents also acts to reduce the amplitude of surge motion. These observations are believed to be due to the offset imposed by the currents and a damping effect from the turbine.

In the wave-only cases, the pitch motion is relatively sinusoidal with the turbine included but exhibits some slight asymmetry without. With the currents included, the pitch motion displays increased high-order behaviour in both the unloaded and loaded cases.

Mooring loads

Figure 3 shows time series data for the total tension in a bow (A) and aft (B) mooring line for each of the cases considered (only results for a single line are plotted as the case is symmetrical).

In both the current-only and combined cases, the tensions in the bow and aft lines are increased and decreased respectively with the loaded case showing a greater deviation. This is expected as a consequence of the exaggerated offset observed in the surge motion. The presence of the turbine again appears to reduce the amplitude of oscillation as does the addition of currents. This is in keeping with the surge behaviour and is again believed to be due to the surge offset and a damping effect caused by the turbine.

Turbine thrust and power output

Figure 4 shows the total thrust force on the turbine disk (A) and the theoretical power output from the turbine (B) for each of the loaded cases.

The theoretical power, plotted in Figure 3B is given by

$$P = \frac{1}{2} AU_{\infty}^3 C_t (1 - a) \rho \quad (5)$$

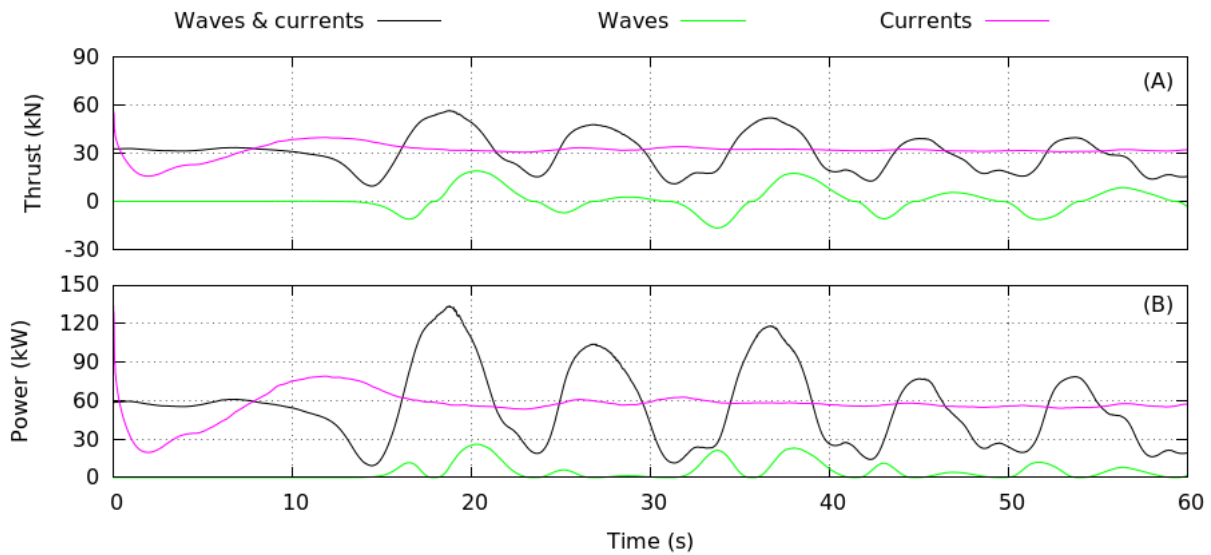


FIGURE 4. TIME SERIES OF THE THRUST ON THE TURBINE (A) AND THE THEORETICAL POWER OUTPUT (B).

which assumes the turbine to be ‘ideal’, i.e. there is no cut-in speed, no maximum power and the turbine is able to operate/generate in flows of either direction. It also assumes that the turbine can instantly react to changes in flow speed. This behaviour can be seen in the wave-only case where the thrust oscillates between positive and negative values providing a power output at approximately twice the frequency of the wave. In reality the SCHOTTEL turbine has a minimum operational flow speed below which no power is generated and the thrust is greatly reduced. It also has a rated flow speed above which the power (and hence the thrust) is limited by an over-speed control strategy.

In the current-only case the turbine model gives a near constant thrust and, hence, power. This shows the model is able to adapt to the local flow conditions. The obtained thrust of $\sim 33\text{kN}$ coincides with that predicted by Equation 3 (assuming a surface flow velocity of 2.8ms^{-1}).

For the combined case both the thrust and power output oscillate, with significant amplitude, around the value found in the current-only case. There is some variation in the amplitudes as well as a higher-order oscillation which appears to coincide with the higher-order behaviour observed in the pitch motion.

CONCLUSIONS

A coupled CFD model has been presented, including waves and currents; fully nonlinear, two-phase fluid dynamics; a floating structure with six degrees of freedom; a 4-point nonlinear catenary mooring system, and; a new two-way coupled actuator disc-type turbine model.

It has been shown that the motion, mooring loads and power delivery, of the floating tidal

stream concept, display considerable complexities beyond simple periodic behaviour. It is clear that, in order to understand the motion of such systems and accurately predict the power output, both currents and waves need to be considered simultaneously. It is also evident that the key elements of these systems are strongly coupled and consequently models that decouple the turbine, barge motion and mooring tensions are likely to have limited predictive capability.

In conclusion, coupled models, such as the one proposed here, including the complete device system and full range of hydrodynamic conditions, are required to understand the behaviour and power delivery of floating tidal stream concepts.

ACKNOWLEDGEMENTS

The authors acknowledge that, this work used the ARCHER UK National Supercomputing Service (<http://www.archer.ac.uk>), is affiliated with the CCP-WSI project (EP/M022382/1) and has been funded as part of Innovate UK Project 102217.

REFERENCES

- [1] Ransley, E., 2015, “Survivability of Wave Energy Converter and Mooring Coupled System using CFD,” Ph.D. thesis, Plymouth University, UK.
- [2] Royal HaskoningDHV, 2014, “Chapter 7: Physical Processes”, in “Perpetuus Tidal Energy Centre (PTEC), Environmental Statement”, Royal HaskoningDHV, Amersfoort, Netherlands.
- [3] Dyer, K. R., 1970, “Current Velocity Profiles in a Tidal Channel,” *Geophys. J. R. astr. Soc.* 22, pp. 153-161.
- [4] Jacobsen, N., Fuhrman, D., and Fredsøe, J., 2012, “A wave generation toolbox for open-source CFD library: OpenFOAM®”, *Int. J. Numer. Meth. Fluids*, 70, pp. 1073-1088.